AIAA JOURNAL
Vol. 47, No. 11, November 2009

Comparison of Direct and Indirect Combustion Noise Mechanisms in a Model Combustor

M. Leyko*
Snecma Groupe SAFRAN, 77550 Moissy-Cramayel, France
F. Nicoud†
Université Montpellier II, 34095 Montpellier, France
and
T. Poinsot‡
Institut de Mécanique des Fluides de Toulouse, 31400 Toulouse, France

DOI: 10.2514/1.43729

Core noise in aeroengines is due to two main mechanisms: direct combustion noise, which is generated by the unsteady expansion of burning gases, and indirect combustion noise, which is due to the acceleration of entropy waves (temperature fluctuations generated by unsteady combustion) within the turbine stages. This paper shows how a simple burner model (a flame in a combustion chamber terminated by a nozzle) can be used to scale direct and indirect noise. An analytical formulation is used for waves generated by combustion. The transmission and generation of waves through the nozzle is calculated using both the analytical results of Marble and Candel (Marble, F. E., and Candel, S., "Acoustic Disturbances from Gas Nonuniformities Convected Through a Nozzle," *Journal of Sound and Vibration*, Vol. 55, 1977, pp. 225–243.) and a numerical tool. Numerical results for the nozzle verify and extend the analytical approach. The analytical relations for the combustion and the nozzle provide simple scaling laws for direct and indirect noise ratio as a function of the Mach number in the combustion chamber and at the nozzle outlet.

Nomenclature

$\mathcal{A}$	=	nozzle cross-sectional area, m^2
$\mathcal{A}_c$	=	throat nozzle cross-sectional area, m^2
$\mathcal{A}_f$	=	combustor cross-sectional area, m^2
c	=	speed of sound, m/s
c_p	=	massic heat capacity at constant pressure, J/K/kg
c_v	=	massic heat capacity at constant volume, J/K/kg
ℓ_f	=	flame length, m
ℓ_n	=	nozzle length, m
$\mathcal{M}$	=	Mach number
$\dot{m}$	=	mass flow rate, kg/s
PW$\{\phi\}$	=	spectral power density of ϕ computed with Welch's method
p	=	thermodynamic pressure, Pa
$\dot{Q}$	=	heat release rate, W
$\dot{q}$	=	heat release rate per volume unit, W/m^3
r	=	massic ideal gas constant, J/K/kg
s	=	massic entropy, J/K/kg
T	=	temperature, K
t	=	time, s
u	=	gas velocity, m/s
w^S	=	dimensionless entropy wave
w^+	=	dimensionless acoustic wave propagating downstream
w^-	=	dimensionless acoustic wave propagating upstream
x	=	x-axis value, m
y	=	y-axis value, m
z	=	z-axis value, m
γ	=	specific heat capacities ratio
δ	=	Dirac distribution
η	=	ratio between indirect and direct noise
ρ	=	mass density, kg/m^3
$\bar{\phi}$	=	temporal mean value of ϕ
ϕ'	=	temporal fluctuation value of ϕ
Ω	=	reduced angular pulsation
ω	=	angular pulsation, rad/s

Subscripts

[AA]	=	acoustic response of the nozzle to an acoustic perturbation
[CC]	=	response of the combustion chamber to a heat release fluctuation
[SA]	=	acoustic response of the nozzle to an entropy perturbation
ϕ_t	=	total quantity of ϕ
ϕ_0	=	quantity ϕ upstream from the combustor
ϕ_1	=	quantity ϕ downstream from the combustor and upstream from the nozzle
ϕ_2	=	quantity ϕ downstream from the nozzle

Received 10 February 2009; revision received 3 July 2009; accepted for publication 4 July 2009.

*Ph.D. Student, Centre Européen de Recherche et de Formation Avancée en Calcul Scientifique, 31057 Toulouse, France; leyko@cerfacs.fr.
†Professor.
‡Research Director, Associate Fellow AIAA.

I. Introduction

OVER the last five decades, jet and external aerodynamic noises of aircraft have been substantially reduced. Further developments will be needed for modern aircraft design in order to meet the increasingly restrictive rules about noise reduction. Although drastic reductions have already been achieved on fan and jet noise, the relative importance of other noise sources has increased and the contribution of these sources must be controlled if further global noise reduction is to be achieved. Among these sources, the noise created by the turbulent flame within the combustor is already identified as nonnegligible at takeoff, especially in the midfrequency range. Two main mechanisms have been identified in the 1970s regarding noise propagation and generation from the combustion chamber to the far field (Fig. 1):

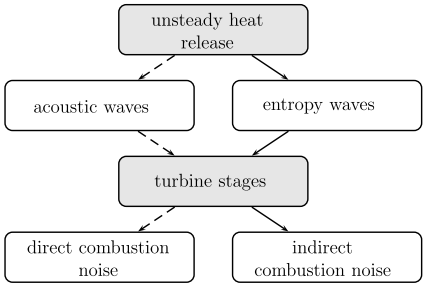

Fig. 1 The two main mechanisms for noise generation from confined flames: direct (dashed line) and indirect (solid line) noise.

1) With direct combustion noise, acoustic perturbations generated by the unsteady heat release from the turbulent flame propagate either upstream or downstream through the turbomachinery stages, where they are distorted by the mean flow, diffracted, and reflected by the solid walls within the diffuser, the distributor, and the turbine and compressor blades.

2) With indirect combustion noise, entropy fluctuations generated within the combustion chambers (hot spots, imperfect mixing, etc.) propagate downstream and interact with accelerating mean flow. The kinematic and thermodynamic variables are strongly coupled when the flow is compressible. Therefore, when there is a sharp variation of the mean flow (turbine stages), mass density fluctuations generate perturbations of the other flow variables. Subsequent acoustic waves are generated and transmitted to the far field through the turbine stages.

Direct combustion noise is typically the main source of noise of a free flame. The acoustic radiation due to a turbulent flame has been theoretically treated by Bragg [1], Strahle [2], Hassan [3], and others. More recently, Ihme et al. [4] successfully computed the sound emitted from a turbulent diffusion flame by combining a large eddy simulation and a computational aeroacoustic method, providing precious information about the combustion-generated noise. The experimental and theoretical work of Candel et al. [5,6] about the noise generated by unsteady laminar flames, as well as the developments of Crighton et al. [7] and the experimental investigations of Rajaram and Lieuwen [8,9] and Lieuwen et al. [10] about combustion-generated noise of turbulent flames, are also an important source of information for direct noise comprehension. However, several studies performed in this field concern the flame acoustic radiation toward the free far field, and in the case of confined systems like aeroengines, another source of noise appears to be relevant: the entropy noise. Indeed, following the work of Tsien [11] and Crocco [12] about nozzles, Candel [13] concludes that entropy spots, inherent to the unsteady combustion process, can represent an important source of noise when considering gas expansion through the engine turbine stages. Candel considers a relative temperature fluctuation of 5% and calculates a corresponding sound pressure level at the nozzle exhaust of about 120 dB. Marble [14] and Marble and Candel [15] obtain solutions for planar waves within compact nozzles and within finite-length nozzles with assumed linear axial-velocity evolution. In the same period, Ffowcs Williams and Howe [16] propose an extended theory for general entropy spots in low Mach number nozzle flows. Stow et al. [17] show that for an annular duct with a nozzle, the relations found by Marble and Candel [15] for compact nozzles apply to the first order even when circumferential modes are present. The compact interactions idea of Marble and Candel was extended to cylindrical 2-D flows by Cumpsty and Marble [18] and applied to commercial aeroengines [19]. Considering that the principal noise mechanism is the indirect one, Cumpsty and Marble presume the relative temperature fluctuation amplitude and spectrum and obtain quite good results for low jet velocities: the so-called excess noise. But Cumpsty and Marble agree to say that although the agreement of the measurements and predictions strongly supports that the indirect noise mechanism is the major core noise generation process, this conclusion is not definitive until a clear separation of the different effects is performed. Starting from the heat release fluctuation, they provide the main ideas to do this analytically, and they briefly comment on the expected results. The aim of the present paper is precisely to develop this work but in a purely one-dimensional (1-D) case.

It should be mentioned that Muthukrishnan et al. [20] experimentally investigated the core noise sources separation and also concluded that for choked nozzles, entropy noise seems to be the main core noise source. More recently, Bake et al. [21–24] worked on the subject, but the separation of direct and indirect combustion noise in a real case is still difficult to evaluate. On one hand, entropy fluctuations are controlled by complicated aerodynamical, thermal, and chemical phenomena. Turbulent mixing and diffusion can also strongly affect entropy wave amplitudes at the nozzle inlet, generally speaking. On the other hand, the acoustic cavity modes of the chamber can also significantly change the acoustic levels [25,26].

In the present study, only the most significant parameters are considered in order to establish simple analytical scaling laws for direct and indirect noise in aeroengines. To compare direct and indirect combustion noise, entropy and acoustic waves will be assumed to be directly linked to heat release fluctuations, and a very simple case of generic combustor is considered: a combustion chamber followed by a nozzle (Fig. 2). The combustion chamber and the turbine stages will be represented by a quasi-1-D system. The combustion zone will be modeled by an infinitely thin heat release fluctuation in a constant section duct (generating acoustic and entropy waves) connected to a quasi-1-D nozzle representing the turbine stages (for the transmission and generation of acoustic waves). These two elements are handled individually, as shown in Fig. 3, and the feedback on the flame of the acoustic waves traveling upward is not taken into account. Thus, the separation between direct and indirect noise is simple to perform because the global system is assumed to be linear. The combustion chamber creates the acoustic and entropy waves feeding the nozzle. The nozzle then generates the outgoing direct or indirect noise depending on the nature of the incoming waves (acoustic or entropy, respectively).

The waves generated by the combustion zone are calculated analytically, considering an isolated heat release fluctuation. This model provides explicitly acoustic and entropy waves for the second

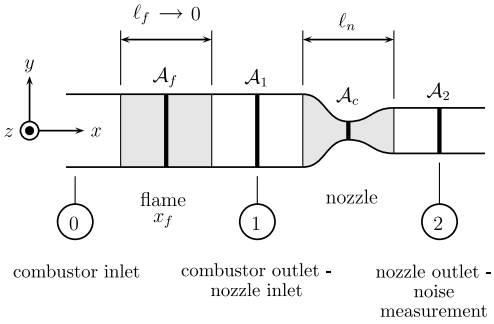

Fig. 2 A generic model to evaluate direct and indirect combustion noise.

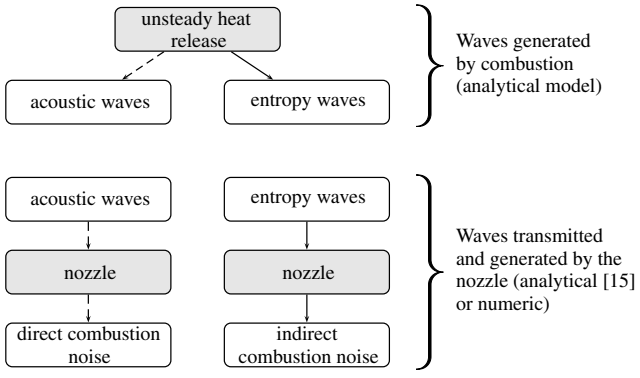

Fig. 3 Strategy for the calculation of the ratio between direct (dashed line) and indirect (solid line) noise.

part of the calculations: the transmission and generation of acoustic waves through the nozzle. The calculation of the transmission of acoustic waves through the nozzle (direct mechanism) and of the generation of acoustic waves from entropy waves within the nozzle (indirect mechanism) is performed both analytically using the results of Marble and Candel [15] for compact nozzles and numerically by solving the Euler equations in the time domain for a 2-D nozzle with a quasi-1-D behavior. The present method thus leads to two main approaches for the calculation of the indirect-to-direct noise ratio: a fully analytical method and a semi-analytical method. In both cases, the calculations of the waves due to combustion and the calculations of the wave transmission and generation through the nozzle are independent.

The analytical calculations of acoustic and entropy waves generated by combustion will be first reviewed in Sec. II. The acoustic wave transmission and generation by the nozzle, obtained analytically and numerically, are then presented in Sec. III. Finally, the ratio between direct and indirect noise is presented in Sec. IV.

II. Acoustic and Entropy Wave Generation in the Combustion Chamber

A subsonic flow is assumed in the combustion region. Viscous and three-dimensional (3-D) effects are neglected and a 1-D heat release region is assumed to represent the combustion zone. The flow is defined with the mass density ρ, the velocity u, and the heat release $\dot{Q}(t)$. The flame length ℓ_f is assumed to be small compared with the acoustic and entropy wavelengths, so that the heat release per unit volume $\dot{q}$ can be expressed as

$$\dot{q}(x, y, z, t) = \delta(x - x_f)\dot{Q}(t)/\mathcal{A}_f \tag{1}$$

where δ is the Dirac distribution and $\mathcal{A}_f$ is the cross-sectional area of the combustion chamber. The heat release $\dot{Q}(t)$ results from the following space integration of $\dot{q}(x, y, z, t)$:

$$\dot{Q}(t) = \iiint_{-\infty}^{+\infty} \dot{q}(x, y, z, t)\,\mathrm{d}x\,\mathrm{d}y\,\mathrm{d}z \tag{2}$$

The steady heat release of the flame model is considered negligible (cold flame) so that the mean flow is assumed isentropic. The cold flame assumption has been used by many authors to obtain analytical scaling regarding thermoacoustic instabilities [27], but it can have a nonnegligible effect as shown by Dowling [28], which is ignored here. The flow is characterized by the mass flow $\dot{m}$, the total enthalpy h_t, and the entropy s. The mass flow $\dot{m}$ and the entropy s can be written as follows:

$$\dot{m} = \rho u \mathcal{A} \tag{3}$$

$$s = c_v \ln\left(\frac{p}{\rho^\gamma}\right) \tag{4}$$

or for small temporal perturbations,

$$\frac{\dot{m}'}{\bar{\dot{m}}} = \frac{1}{\bar{\mathcal{M}}}\frac{u'}{\bar{c}} + \frac{p'}{\gamma\bar{p}} - \frac{s'}{c_p} \tag{5}$$

and

$$\frac{s'}{c_p} = \frac{p'}{\gamma\bar{p}} - \frac{\rho'}{\bar{\rho}} \tag{6}$$

Heat capacities and the composition of the gas are assumed to be constant, so that the total enthalpy is defined by $h_t = c_p T_t$, where T_t is the total temperature:

$$T_t = T\left(1 + \frac{\gamma - 1}{2}\mathcal{M}^2\right) \tag{7}$$

The fluctuation of the Mach number $\mathcal{M}$ is:

$$\frac{\mathcal{M}'}{\bar{\mathcal{M}}} = \frac{1}{\bar{\mathcal{M}}}\frac{u'}{\bar{c}} - \frac{\gamma - 1}{2}\frac{p'}{\gamma\bar{p}} - \frac{1}{2}\frac{s'}{c_p} \tag{8}$$

The fluctuations of total temperature as a function of velocity, pressure, and entropy perturbations can be written using Eqs. (6) and (8), and the state equation for small perturbations:

$$\frac{T_t'}{\bar{T}_t} = \frac{1}{1 + [(\gamma - 1)/2]\bar{\mathcal{M}}^2}\left[(\gamma - 1)\bar{\mathcal{M}}\frac{u'}{\bar{c}} + (\gamma - 1)\frac{p'}{\gamma\bar{p}} + \frac{s'}{c_p}\right] \tag{9}$$

To scale direct and indirect combustion noise, the dimensionless acoustic waves (w^+ and w^-) and the entropy wave (w^S) created by the compact flame of the combustion chamber must be assessed. These waves are defined as follows:

$$w^+ = \frac{p'}{\gamma\bar{p}} + \frac{u'}{\bar{c}} \tag{10}$$

$$w^- = \frac{p'}{\gamma\bar{p}} - \frac{u'}{\bar{c}} \tag{11}$$

$$w^S = \frac{p'}{\gamma\bar{p}} - \frac{\rho'}{\bar{\rho}} \tag{12}$$

The wave w^+ is related to the propagation speed $u + c$, whereas the wave w^- is related to the propagation speed $u - c$. The wave w^S propagates at the convective speed u and transports entropy.

Considering the heat release $\dot{Q}$ through the heating region according to Fig. 4, the balance equations of mass flow, total enthalpy, and entropy at the flame front yield

$$(\dot{m})_0 = (\dot{m})_1 \tag{13}$$

$$(\dot{m}h_t)_0 + \dot{Q} = (\dot{m}h_t)_1 \tag{14}$$

$$(\dot{m}s)_0 + \frac{\dot{Q}}{\bar{T}} = (\dot{m}s)_1 \tag{15}$$

where the subscripts 0 and 1 correspond, respectively, to the quantities upstream and downstream from the flame. The mean heat release is zero, so that the mean temperature $\bar{T}$, Mach number $\bar{\mathcal{M}}$, total temperature $\bar{T}_t$, and entropy $\bar{s}$ do not change through the flame model. For small temporal perturbations, using the mass flow balance equation (13), the entropy balance equation (15) leads to

$$\left(\frac{s'}{c_p}\right)_0 + \frac{\dot{Q}'}{\bar{\dot{m}}c_p\bar{T}} = \left(\frac{s'}{c_p}\right)_1 \tag{16}$$

Equation (14) can be modified in the same way; using the expression of the fluctuations of the total temperature in Eq. (9), the total enthalpy balance equation (14) for small temporal perturbations leads to

$$\begin{aligned}(\gamma - 1)\bar{\mathcal{M}}\left(\frac{u'}{\bar{c}}\right)_0 + (\gamma - 1)\left(\frac{p'}{\gamma\bar{p}}\right)_0 + \left(\frac{s'}{c_p}\right)_0 + \frac{\dot{Q}'}{\bar{\dot{m}}c_p\bar{T}} \\ = (\gamma - 1)\bar{\mathcal{M}}\left(\frac{u'}{\bar{c}}\right)_1 + (\gamma - 1)\left(\frac{p'}{\gamma\bar{p}}\right)_1 + \left(\frac{s'}{c_p}\right)_1\end{aligned} \tag{17}$$

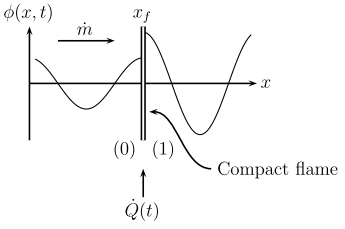

Fig. 4 Compact flame illustration regarding a quantity ϕ upstream (0) and downstream (1) from the heating region.

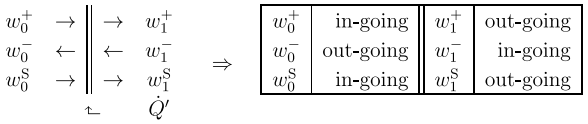

Fig. 5 Incoming and outgoing waves for the compact flame.

The heat release is supposed to be known, and the three incoming waves have to be imposed in order to obtain the outgoing waves w_1^+, w_1^S, and w_0^- using the three balance equations (13–15) as a function of the heat release (Fig. 5) . Except for the heat release, the combustor is assumed to be isolated; that is to say, the incoming acoustic waves w_0^+ and w_1^- are equal to zero as well as the incoming entropy wave w_0^S. Considering the last assumption $w_0^S = 0$ and using Eq. (16), the outgoing entropy w_1^S can be expressed as

$$w_1^S = \frac{\dot{Q}'}{\bar{\dot{m}} c_p \bar{T}} \tag{18}$$

The fluctuation of the mass flow equation (5) can be written at the upstream (0) and downstream (1) from the flame and expressed as a function of waves instead of the fluctuations of velocity, pressure, and entropy. Then, Eq. (17) (related to the fluctuations of total enthalpy) can also be written as a function of waves. Using Eq. (18) and the assumption that the flame is isolated ($w_0^+ = 0$, $w_1^- = 0$, and $w_0^S = 0$), one can show that the expression of the outgoing acoustic wave w_1^+ generated by the heat release fluctuation is

$$w_1^+ = \frac{\bar{\mathcal{M}}}{1 + \bar{\mathcal{M}}} \frac{\dot{Q}'}{\bar{\dot{m}} c_p \bar{T}} \tag{19}$$

Finally, Eqs. (18) and (19) lead to the ratio between the acoustic wave w_1^+ and the entropy wave w_1^S generated by the combustion zone and propagating downstream of the combustion chamber:

$$\frac{w_1^+}{w_1^S}[\mathrm{CC}] = \frac{\bar{\mathcal{M}}}{1 + \bar{\mathcal{M}}} \tag{20}$$

where [CC] refers to the waves produced in the combustion chamber. Equation (20) shows that, for a compact flame, the ratio between acoustic and entropy waves depends only on the Mach number in the flame zone $\bar{\mathcal{M}}$ and no more on the heat release fluctuations. This result allows study of the ratio between indirect and direct combustion noise mechanisms independently of the exact nature of heat release fluctuations, which are the sources of each mechanism.

III. Wave Transmission and Generation Through a Nozzle

The transmission and generation of acoustic and entropy waves through the nozzle are obtained using two different methods. The first one is based on the analytical development of Marble and Candel [15], assuming that the nozzle is compact (frequency is low). In their work, the authors assume a quasi-1-D nozzle flow and quasi-steady perturbations of mass flow, energy, and entropy leading to relations between the different waves that depend on the inlet and outlet Mach numbers. This approach is similar to the one used for the compact flame of Sec. II, and the relations between waves for the nozzle are reviewed in the first part of this section. The second method to obtain the acoustic response of the nozzle is based on a numerical simulation of the quasi-1-D nozzle flow by solving the Euler equations [29]. This second method is valid for all frequencies as long as the waves remain 1-D, and it will be used here to evaluate the compact nozzle assumption of the analytical approach in the low-frequency limit. The numerical approach is presented in the second part of this section.

A. Analytical Approach

Following the analysis of Marble and Candel [15], the flow is supposed to be 1-D. Similar to Sec. II, u stands for the axial velocity,

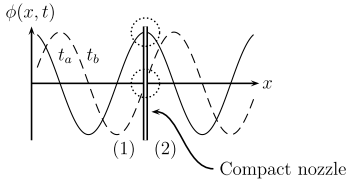

Fig. 6 Compact nozzle illustration. The quantity ϕ, conserved throughout the nozzle, is the same upstream (1) and downstream (2) at each instant.

ρ for the mass density, and $\mathcal{A}$ for the nozzle cross-sectional area. The mass flow $\dot{m}$ and the entropy s are defined by Eqs. (3) and (4). Assuming that the nozzle is isolated, the total enthalpy is conserved, and thus the total temperature also. Note that the total temperature T_t is, in this case, always conserved, even for a nonisentropic mean flow in the nozzle (which is to say, through a shock, for instance). The total temperature is defined by Eq. (7) and the expression of the fluctuations of total temperature entering the nozzle as a function of speed, pressure, and entropy perturbations is the same as in Sec. II [Eq. (9)]. Under the assumption of a compact nozzle [long wavelengths compared with the nozzle length ℓ_n (see Fig. 6)], there is no delay or distortion between the inlet and the outlet of the nozzle. As a result, mass flow, total temperature, and entropy are conserved through the nozzle. The quantities upstream and downstream from the nozzle are, respectively, subscripted 1 and 2. The conservation equations (5), (6), and (9) can be written as a system of equations which are functions only of the Mach numbers and the waves (acoustic and entropy) upstream and downstream of the nozzle. This system is composed of three equations involving six waves, thus the incoming waves have to be imposed. In the case of an unchoked nozzle, the flow is totally subsonic and the w_2^- wave is incoming so that waves w_1^+, w_1^S, and w_2^- can be imposed (Fig. 7). Finally, the system is composed of three equations and three unknown waves. Because the system is linear, mechanisms can be separated by setting $w_1^+ \neq 0$, $w_1^S = 0$, and $w_2^- = 0$ in a first step to study only the acoustic response of the nozzle to an acoustic perturbation. This case is called [AA]. It is also possible to set $w_1^+ = 0$, $w_1^S \neq 0$, and $w_2^- = 0$ in order to study the acoustic response of the nozzle to an entropy perturbation, and this case is called [SA]. Using Eqs. (5), (6), and (9) at the inlet and the outlet of the nozzle for the cases [AA] and [SA] gives

$$\frac{w_2^+}{w_1^+}[\mathrm{AA}] = \frac{2\bar{\mathcal{M}}_2}{1 + \bar{\mathcal{M}}_2} \frac{1 + \bar{\mathcal{M}}_1}{\bar{\mathcal{M}}_1 + \bar{\mathcal{M}}_2} \frac{1 + [(1/2)(\gamma - 1)]\bar{\mathcal{M}}_2^2}{1 + [(1/2)(\gamma - 1)]\bar{\mathcal{M}}_1\bar{\mathcal{M}}_2} \tag{21}$$

$$\frac{w_2^+}{w_1^S}[\mathrm{SA}] = \frac{\bar{\mathcal{M}}_2 - \bar{\mathcal{M}}_1}{1 + \bar{\mathcal{M}}_2} \frac{(1/2)\bar{\mathcal{M}}_2}{1 + [(1/2)(\gamma - 1)]\bar{\mathcal{M}}_1\bar{\mathcal{M}}_2} \tag{22}$$

In the case of an isentropic choked nozzle, the flow is subsonic in the convergent part of the nozzle and totally supersonic in the divergent part, and wave w_2^- cannot be imposed because it is outgoing (Fig. 8). In the case of an isentropic choked nozzle, only two waves can be imposed so that the system is composed of four unknown waves for three equations only. The missing equation is obtained by stating that the flow at the nozzle throat is sonic so that the relation between the Mach number $\mathcal{M}$ and the cross-sectional area ratio can be written as follows:

$$\frac{\mathcal{A}}{\mathcal{A}_c} = \frac{1}{\mathcal{M}} \left[\frac{2}{\gamma + 1} \left(1 + \frac{\gamma - 1}{2} \mathcal{M}^2 \right) \right]^{(1/2)[(\gamma+1)/(\gamma-1)]} \tag{23}$$

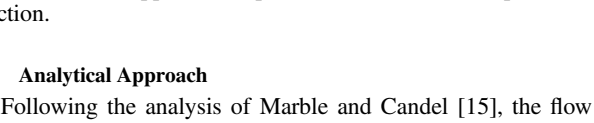

Fig. 7 Incoming and outgoing waves for the unchoked nozzle case.

$$\begin{array}{ccc||ccc} w_1^+ & \rightarrow & \| & \rightarrow & w_2^+ \\ w_1^- & \leftarrow & \| & \rightarrow & w_2^- \\ w_1^S & \rightarrow & \| & \rightarrow & w_2^S \end{array} \quad \Rightarrow \quad \begin{array}{|c|c||c|c|} \hline w_1^+ & \text{in-going} & w_2^+ & \text{out-going} \\ w_1^- & \text{out-going} & w_2^- & \text{out-going} \\ w_1^S & \text{in-going} & w_2^S & \text{out-going} \\ \hline \end{array}$$

Fig. 8 Incoming and outgoing waves for the choked nozzle case.

where $\mathcal{A}_c$ is the cross-sectional area at the nozzle throat. One can easily show from Eq. (23) that for the choked nozzle case, the temporal fluctuation of the Mach number $\mathcal{M}'/\bar{\mathcal{M}}$ is zero. Then, using the expression of the fluctuation of the Mach equation (8),

$$\frac{1}{\bar{\mathcal{M}}}\frac{u'}{\bar{c}} - \frac{\gamma-1}{2}\frac{p'}{\gamma\bar{p}} - \frac{1}{2}\frac{s'}{c_p} = 0 \tag{24}$$

The entropy s and the total temperature T_t are constant through the nozzle, so that the total pressure p_t is also constant. The total pressure can be expressed as follows:

$$p_t = p\left(1 + \frac{\gamma-1}{2}\mathcal{M}^2\right)^{\gamma/(\gamma-1)} \tag{25}$$

The temporal fluctuation of total pressure of Eq. (25) can be written:

$$\frac{p_t'}{\bar{p}_t} = \frac{p'}{\bar{p}} + \frac{\gamma\bar{\mathcal{M}}^2}{1+[(\gamma-1)/2]\bar{\mathcal{M}}^2}\frac{\mathcal{M}'}{\bar{\mathcal{M}}} \tag{26}$$

and shows that the fluctuations $p'/(\gamma\bar{p})$ are the same on both sides of the nozzle because the Mach number fluctuation is zero:

$$\left(\frac{p'}{\gamma\bar{p}}\right)_1 = \left(\frac{p'}{\gamma\bar{p}}\right)_2 \tag{27}$$

Finally, Eqs. (6), (24), and (27) used at the inlet and outlet of the nozzle yield

$$\frac{w_2^+}{w_1^+}[\text{AA}] = \frac{1+[(1/2)(\gamma-1)]\bar{\mathcal{M}}_2}{1+[(1/2)(\gamma-1)]\bar{\mathcal{M}}_1} \tag{28}$$

$$\frac{w_2^+}{w_1^S}[\text{SA}] = \frac{(1/2)(\bar{\mathcal{M}}_2 - \bar{\mathcal{M}}_1)}{1+[(1/2)(\gamma-1)]\bar{\mathcal{M}}_1} \tag{29}$$

The set of equations (21), (22), (28), and (29) provides analytical expressions for the outgoing waves w_2^+ as a function of the incoming waves w_1^+ and w_1^S and the mean inlet $\bar{\mathcal{M}}_1$ and outlet $\bar{\mathcal{M}}_2$ Mach numbers for the compact nozzle.

B. Numerical Approach

The previous analytical relations are based on the nozzle compactness assumption and are valid only for the low-frequency limit. To validate this assumption and extend the model for the nozzle to a larger range of frequencies, an unsteady simulation based on Euler equations of the flow within the nozzle has been performed. Acoustic and entropy perturbations are generated at the inlet of the computational domain in a simple 1-D isentropic nozzle flow, and outgoing noise is directly measured in the simulation.

1. *Numerical Method*

The numerical tool used to solve the flow within the nozzle is the AVBP [30,31] code. AVBP is a finite volume cell-vertex code that can solve 3-D compressible Navier–Stokes equations on unstructured meshes, but it is used here on a 2-D regular mesh without viscous terms. The mesh is two-dimensional (2-D) [476×5 with 320 nodes in the nozzle (see Fig. 9)] and the evolution of the transversal coordinate is small enough to assume that the flow in the nozzle is quasi-1-D. There are about 320 nodes in the axial direction of the nozzle. The numerical computations have been performed with the Lax–Wendroff scheme, which is second-order accurate in both space and time, with a Courant–Friedrichs–Lewy number of 0.5. Preliminary tests performed with the same solver on acoustic and entropy wave propagation were used to verify that the results were independent of the mesh and that dispersion and dissipation errors were very small.

2. *Nozzle Geometry and Flow Parameters*

Because an inviscid 1-D and compressible flow is also considered in the simulation, the mean Mach numbers $\bar{\mathcal{M}}_1$ and $\bar{\mathcal{M}}_2$ only depend on the cross-sectional area ratio $\mathcal{A}_1/\mathcal{A}_2$ for the unchoked nozzle case, and on the cross-sectional area ratios $\mathcal{A}_1/\mathcal{A}_c$ and $\mathcal{A}_2/\mathcal{A}_c$ for the isentropic choked nozzle case [see Eq. (23)]. For the choked nozzle case, the nozzle is convergent and divergent, whereas it is simply convergent for the unchoked nozzle case. To calculate the section area ratio $\mathcal{A}_1/\mathcal{A}_2$ for the unchoked case, the following relation is used:

$$\frac{\mathcal{A}_1}{\mathcal{A}_2} = \frac{\bar{\mathcal{M}}_2}{\bar{\mathcal{M}}_1}\left[\frac{1+[(\gamma-1)/2]\bar{\mathcal{M}}_1^2}{1+[(\gamma-1)/2]\bar{\mathcal{M}}_2^2}\right]^{[(1/2)(\gamma+1)/(\gamma-1)]} \tag{30}$$

The different values of cross-sectional area ratios used in the present work are presented in Table 1 as a function of inlet Mach number $\bar{\mathcal{M}}_1$ and outlet Mach number $\bar{\mathcal{M}}_2$ for a specific heat capacities ratio γ of 1.32. The static pressure and temperature are imposed at the inlet of the nozzle ($p_1 = 800.0$ kPa, $T_1 = 1300$ K) and are the same for all cases. The static pressure p_2 is also imposed at the outlet and is chosen to obtain an isentropic flow and thus the correct target Mach numbers.

3. *Numerical Boundary Conditions and Computations*

Like in the analytical approach, the acoustic response of the nozzle at the outlet is computed for a case in which the incoming waves pulsed at the nozzle inlet are entropy (case [SA]) and for a case in which the waves are acoustic (case [AA]). In this numerical computation, totally nonreflecting boundary conditions are imposed (w_1^+ independent of w_1^- at the nozzle inlet and $w_2^- = 0$ for the subsonic nozzle outlet case) and the desired incoming perturbation added [31,32]. The incoming waves at the nozzle inlet are imposed as follows:

$$\begin{cases} w_1^S(t) = n(t) \\ w_1^+(t) = 0 \end{cases}$$

for the case [SA] and

$$\begin{cases} w_1^S(t) = 0 \\ w_1^+(t) = n(t) \end{cases}$$

for the case [AA], where $n(t)$ is a filtered white noise signal. The perturbations $n(t)$ are small enough to neglect nonlinear effects. As a result, one single computation with a filtered white noise signal imposed at the inlet can be performed to obtain the acoustic response of the nozzle to a large range of frequencies. The cutoff frequency of the filtered white noise signal and the size of the biggest cell are chosen in order to solve the smallest wavelength over 20 nodes in the most unfavorable case, that is to say, when the entropy waves are pulsed and when the Mach numbers are small. The smallest acoustic wave length taken into account here is of the order of half the nozzle length (this corresponds to about one-sixteenth of the nozzle length for the entropy wave in the most unfavorable case). However, to avoid border effects in the frequency domain due to the low-pass filter and to have a better numerical precision in the range of interest,

Fig. 9 Mesh of the nozzle corresponding to the case with $\mathcal{M}_1 = 0.050$ and $\mathcal{M}_2 = 1.600$.

Table 1 Geometric cross-sectional area ratio values for the different Mach number cases

	Unchoked cases		Choked cases	
	$\bar{\mathcal{M}}_2 = 0.400$	$\bar{\mathcal{M}}_2 = 0.800$	$\bar{\mathcal{M}}_2 = 1.200$	$\bar{\mathcal{M}}_2 = 1.600$
$\bar{\mathcal{M}}_1 = 0.025$				
$\mathcal{A}_1/\mathcal{A}_c$	14.604	22.482	23.365	23.365
$\mathcal{A}_2/\mathcal{A}_c$	1.000	1.000	1.032	1.267
$\bar{\mathcal{M}}_1 = 0.050$				
$\mathcal{A}_1/\mathcal{A}_c$	7.310	11.253	11.695	11.695
$\mathcal{A}_2/\mathcal{A}_c$	1.000	1.000	1.032	1.267
$\bar{\mathcal{M}}_1 = 0.100$				
$\mathcal{A}_1/\mathcal{A}_c$	3.671	5.651	5.873	5.873
$\mathcal{A}_2/\mathcal{A}_c$	1.000	1.000	1.032	1.267

the results presented in the next section are given for a reduced frequency range. The upper frequency limit of the presented results corresponds to a grid resolution of 50 nodes for the smallest entropy wavelength.

Temporal evolutions of the different waves are recorded at the nozzle inlet and outlet, and the Welch's method [33] is used to compute the spectral power density of the wave signals and thus establish the desired spectral transfer functions. A first computation (case [SA]) provides the transfer function:

$$\sqrt{\mathrm{PW}\{w_2^+\}/\mathrm{PW}\{w_1^S\}}$$

relevant of the indirect mechanism, whereas a second computation (case [AA]) provides the transfer function:

$$\sqrt{\mathrm{PW}\{w_2^+\}/\mathrm{PW}\{w_1^+\}}$$

relevant of the direct mechanism. These numerical transfer functions of the nozzle, in combination with the analytical results for waves generated by the combustion zone, are then used to calculate the semi-analytic indirect-to-direct ratio.

IV. Results

Results of Sec. II and III are used to calculate the ratio η between amplitude $w^+_{2,\mathrm{ind}}$ of the acoustic wave generated indirectly and the amplitude $w^+_{2,\mathrm{dir}}$ of the acoustic wave generated directly as described in Fig. 10. The acoustic wave $w^+_{2,\mathrm{ind}}$ generated by the indirect mechanism is expressed using the entropy wave w_1^S[CC] produced by the flame and the transfer function of the nozzle of the case [SA]. The acoustic wave $w^+_{2,\mathrm{dir}}$ generated by the direct mechanism is, however, expressed using the acoustic wave w_1^+[CC] produced by the flame and the transfer function of the nozzle of the case [AA]. The ratio η is defined as follows:

$$\eta = \frac{w^+_{2,\mathrm{ind}}}{w^+_{2,\mathrm{dir}}} \tag{31}$$

where

$$w^+_{2,\mathrm{dir}} = \frac{w_2^+}{w_1^+}[\mathrm{AA}] \cdot w_1^+[\mathrm{CC}] \tag{32}$$

and

$$w^+_{2,\mathrm{ind}} = \frac{w_2^+}{w_1^S}[\mathrm{SA}] \cdot w_1^S[\mathrm{CC}]$$

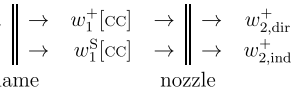

Fig. 10 Definition of the direct and indirect acoustic waves.

The ratio η can be calculated, as mentioned previously, either in a fully analytic [using the analytical relations of Marble and Candel [15] for the transmission and generation of waves through a compact nozzle and the analytic relation for waves generated by combustion (Sec. III.A)] or a semi-analytic manner [using the numerical calculations for the transmission and generation of waves through 1-D nozzle flow and the same analytical relation for waves generated by combustion (Sec. III.B)]:

$$\eta = \underbrace{\frac{w_2^+}{w_1^S}[\mathrm{SA}]}_{\text{analytic or numeric}} \underbrace{\frac{w_1^S}{w_1^+}[\mathrm{CC}]}_{\text{analytic}} \underbrace{\frac{w_1^+}{w_2^+}[\mathrm{AA}]}_{\text{analytic or numeric}} \tag{33}$$

The fully analytic expression of the ratio η is established using Eq. (20), which gives the ratio between acoustic and entropy waves produced by the combustion chamber (case [CC]), and Eqs. (21), (22), (28), and (29), which give the transmitted and generated waves by a compact nozzle (cases [SA] and [AA]. For this approach, the expression of η is

$$\eta = \frac{1}{\bar{\mathcal{M}}_1} \frac{(\bar{\mathcal{M}}_2 - \bar{\mathcal{M}}_1)(\bar{\mathcal{M}}_2 + \bar{\mathcal{M}}_1)}{2(1 + \frac{1}{2}(\gamma - 1)\bar{\mathcal{M}}_2^2)} \tag{34}$$

for the unchoked nozzle and

$$\eta = \frac{1 + \bar{\mathcal{M}}_1}{\bar{\mathcal{M}}_1} \frac{\bar{\mathcal{M}}_2 - \bar{\mathcal{M}}_1}{2(1 + \frac{1}{2}(\gamma - 1)\bar{\mathcal{M}}_2)} \tag{35}$$

for the choked nozzle.

The ratios between indirect and direct noise η calculated with the fully analytic and semi-analytic approaches are plotted hereafter for the Mach numbers defined previously, as a function of reduced pulsation $\Omega = \omega \ell_n / \bar{c}_1$ related to the pulsation ω, the speed of sound at the nozzle inlet $\bar{c}_1$, and the nozzle length ℓ_n. Figure 11 shows that for this simple case, the indirect combustion noise is globally in the same range of magnitude as the direct one; it can be even 10 times greater in the most unfavorable case (low inlet Mach number and high outlet Mach number). The ratio between indirect and direct noise in Fig. 11 is plotted versus the dimensionless pulsation Ω. The parameter $\Omega(\omega \ell_n / \bar{c}_1)$ corresponds to the acoustically reduced pulsation and quantifies the acoustic compactness of the nozzle. To be representative of the entropy compactness of the nozzle, this dimensionless pulsation simply needs to be divided by the Mach number at the nozzle inlet. That is to say, the nozzle is 10 (inlet Mach number 0.1) to 40 (inlet Mach number 0.025) times less compact from an entropy point of view than acoustically. For reduced pulsations going to zero (compact nozzle assumption), the numerical computations converge to the ratio η calculated with the analytical relations for the nozzle established by Marble and Candel [15]. Figure 11 shows that the slope of η for $\Omega = 0$ is close to zero, so that the analytical expression remains valid (less than 20% error) up to $\Omega = 0.2$ in most cases, that is to say, even when the entropy wavelength is of the order of the nozzle length. The fully analytic approach thus provides a good idea of what the indirect-to-direct ratio can be.

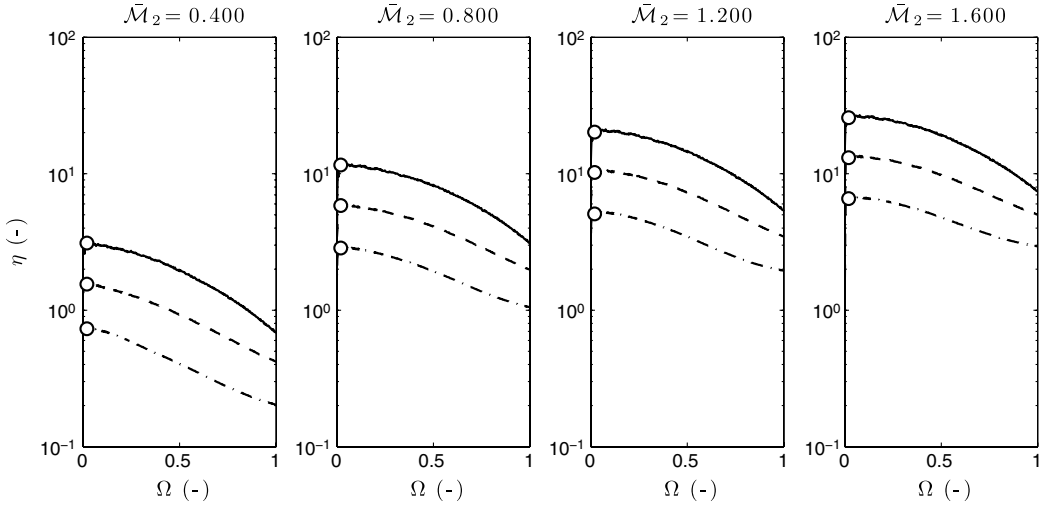

Fig. 11 Estimation of the ratio η between indirect and direct noise. Chain dotted line Mach number $\bar{\mathcal{M}}_1 = 0.100$, dotted line Mach number $\bar{\mathcal{M}}_1 = 0.050$, and solid line Mach number $\bar{\mathcal{M}}_1 = 0.025$. All curves correspond to the semi-analytic method. Circles give the analytic solution for low frequencies [Eqs. (34) and (35)].

This ratio calculated with the fully analytic approach is plotted versus the nozzle inlet and outlet Mach numbers in Fig. 12. Nowadays, the overall pressure ratio at takeoff for commercial aeroengines ranges from about 30 to 40, which is equivalent to an acceleration leading to an outlet Mach number of about 2.0. This graph shows that for an outlet Mach number between unity and two and an inlet Mach number close to 0.05 (a condition which can be found in aeroengines), the indirect combustion noise can be more than 10 times as important as the direct one. Equation (35) shows that when the outlet Mach number $\bar{\mathcal{M}}_2$ is high, the ratio η depends only on the inlet Mach number $\bar{\mathcal{M}}_1$ and tends to $(1 + \bar{\mathcal{M}}_1)/\bar{\mathcal{M}}_1(\gamma - 1)$. With the previous value of the inlet Mach number of 0.05, the maximum ratio η is then greater than 60. Of course, the present estimation is quite oversimplified because, in a real engine, the strong azimuthal deviation of flow within the turbine stages have to be taken into account as well as the blade loading and blade rows spacing. This approach has been followed by Cumpsty and Marble [18,19], but the number of parameters involved in such a method is important and the results are engine dependent (even if general designs can be used to perform such a calculation). The present approach provides a simple method for the estimation of the indirect-to-direct noise ratio and confirms the importance of indirect noise.

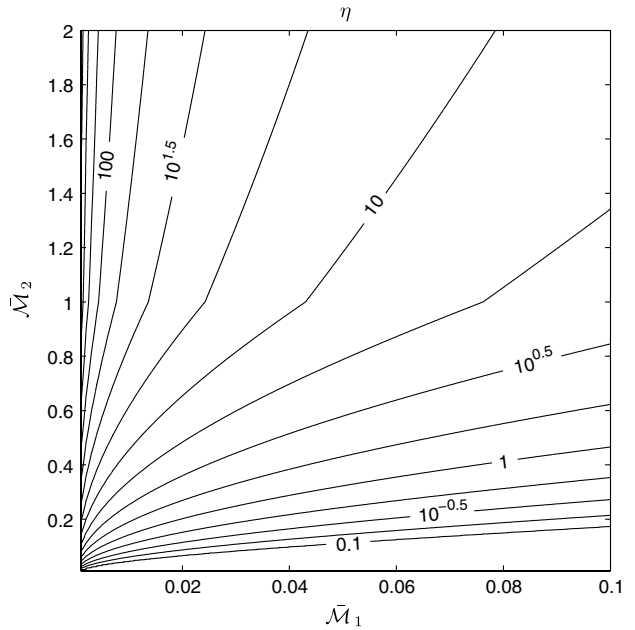

Fig. 12 Ratio η between indirect and direct noise calculated by the fully analytic approach. $\bar{\mathcal{M}}_1$ is the Mach number in the combustion chamber and at the nozzle inlet, and $\bar{\mathcal{M}}_2$ is the Mach number at the nozzle outlet.

V. Conclusions

The noise produced by an aeroengine is generated either by the acoustic waves created by unsteady combustion (direct noise) or by the entropy waves created by combustion and convected through the turbine stages, where they create noise (indirect noise). A simple quasi-1-D combustor model, based on a combustion chamber terminated by a nozzle, has been used to evaluate all waves (acoustic and entropy) created by an unsteady flame zone and to quantify direct and indirect noise. Wave propagation in this model can be determined in the low-frequency limit using fully analytical methods as suggested by Marble and Candel [15] or for all frequencies using a semi-analytical-numerical technique in which the wave propagation through the nozzle is solved using the Euler equations while the rest of the problem is handled analytically. Results demonstrate that the analytical approximation remains valid up to the acoustically reduced pulsations of order of 0.2 (that is to say, even when the entropy wavelength is of the order of the nozzle length) for the given range of inlet Mach numbers (0.025–0.100). They also show that the ratio of indirect-to-direct noise depends on two Mach numbers: the Mach number in the flame zone and the Mach number at the nozzle outlet. This ratio should be small for laboratory experiments but large in most real aeroengines, showing that research on combustion noise needs to incorporate indirect noise generation.

Acknowledgments

This work was partly funded by the Fondation de Recherche pour l'Aéronautique et l'Espace and the Direction Générale de l'Aviation Civile, within the BRUCO (bruit de combustion issu des turbines à gaz) project and the AITEC (analyse instationnaire des turbomachines en aerodynamique et acoustique) research program, respectively. The authors gratefully acknowledge support from the Centre Informatique National de l'Enseignement Supérieur for the access to computing resources. N. Lamarque is thanked for questions and discussions on theoretical backgrounds. F. Duchaine and A. Roux are thanked for their support about computational issues.

References

[1] Bragg, S., "Combustion Noise," *Journal of Institute of Fuel*, Vol. 36, No. 264, 1963, pp. 12–16.

[2] Strahle, W., "Combustion Noise," *Progress in Energy and Combustion Science*, Vol. 4, No. 3, 1978, pp. 157–176.

[3] Hassan, H. A., "Scaling of Combustion-Generated Noise," *Journal of Fluid Mechanics*, Vol. 66, No. 3, 1974, pp. 445–453. doi:10.1017/S0022112074000292

[4] Ihme, M., Pitsch, H., and Bodony, D., "Radiation of Noise in Turbulent Non-Premixed Flames," *Proceedings of the Combustion Institute*, Vol. 32, No. 1, 2009, pp. 1545–1553. doi:10.1016/j.proci.2008.06.137

[5] Candel, S., Durox, D., and Schuller, T., "Flame Interactions as a Source of Noise and Combustion Instabilities," 10th AIAA/CEAS Aeroacoustics Conference, AIAA Paper 2004-2928, 2004.

[6] Candel, S., Durox, D., Ducruix, S., Birbaud, A.-L., Noiray, N., and Schuller, T., "Flame Dynamics and Combustion Noise: Progress and Challenges," *11th CEAS-ASC Workshop and 2nd Scientific Workshop of X3-Noise: Experimental and Numerical Analysis and Prediction of Combustion Noise*, Inst. Superior Tecnico, Lisbon, 2007.

[7] Crighton, D. G., Dowling, A. P., Ffowcs Williams, J. E., Heckl, M., and Leppington, F., *Modern Methods in Analytical Acoustics: Lecture Notes*, Springer–Verlag, New York, 1992.

[8] Rajaram, R., and Lieuwen, T., "Parametric Studies of Acoustic Radiation from Turbulent Premixed Flames," *Combustion Science and Technology*, Vol. 175, No. 12, 2003, pp. 2269–2298.

[9] Rajaram, R., and Lieuwen, T., "Effect of Approach Flow Turbulence Characteristics on Sound Generation from Premixed Flames," 42nd AIAA Aerospace Sciences Meeting and Exhibit, AIAA Paper 2004-0461, 2004.

[10] Lieuwen, T., Mohan, S., Rajaram, R., and Preetham, "Acoustic Radiation from Weakly Wrinkled Premixed Flames," *Combustion and Flame*, Vol. 144, Nos. 1–2, 2006, pp. 360–369. doi:10.1016/j.combustflame.2005.08.004

[11] Tsien, H. S., "The Transfer Functions of Rocket Nozzles," *Journal of the American Rocket Society*, Vol. 22, No. 3, May–June 1952, pp. 139–143.

[12] Crocco, L., "Supercritical Gaseous Discharge with High Frequency Oscillations," *Aerotechnica*, Vol. 33, No. 1, 1953, pp. 46–53.

[13] Candel, S., "Analytical Studies of Some Acoustic Problems of Jet Engines," Ph.D. Thesis, California Inst. of Technology, Pasadena, CA, 1972.

[14] Marble, F. E., "Acoustic Disturbances from Gas Nonuniformities Convected Through a Nozzle,"*Proceedings of the Interagency Symposium on University Research in Transportation Noise*, Vol. 1, Stanford Univ., Stanford, CA, March 1973.

[15] Marble, F. E., and Candel, S., "Acoustic Disturbances from Gas Nonuniformities Convected Through a Nozzle," *Journal of Sound and Vibration*, Vol. 55, No. 2, 1977, pp. 225–243.

[16] Ffowcs Williams, J. E., and Howe, M. S., "The Generation of Sound by Density Inhomogeneities in Low Mach Number Nozzle Flows," *Journal of Fluid Mechanics*, Vol. 70, No. 3, 1975, pp. 605–622. doi:10.1017/S0022112075002224

[17] Stow, S. R., Dowling, A. P., and Hynes, T. P., "Reflection of Circumferential Modes in a Choked Nozzle," *Journal of Fluid Mechanics*, Vol. 467, No. 1, 2002, pp. 215–239. doi:10.1017/S0022112002001428

[18] Cumpsty, N. A., and Marble, F. E., "The Interaction of Entropy Fluctuations with Turbine Blade Rows: A Mechanism of Turbojet Engine Noise," *Proceedings of the Royal Society of London, Series A: Mathematical and Physical Sciences*, Vol. 357, No. 1960, 1977, pp. 323–344.

[19] Cumpsty, N., and Marble, F., "Core Noise from Gas Turbine Exhausts," *Journal of Sound and Vibration*, Vol. 54, No. 2, 1977, pp. 297–309.

[20] Muthukrishnan, M., Strahle, W., and Neale, D., "Separation of Hydrodynamic, Entropy, and Combustion Noise in a Gas Turbine Combustor," *AIAA Journal*, Vol. 16, No. 4, 1978, pp. 320–327. doi:10.2514/3.60895

[21] Bake, F., Michel, U., Rohle, I., Richter, C., Thiele, F., Liu, M., and Noll, B., "Indirect Combustion Noise Generation in Gas Turbines," 11th AIAA/CEAS Aeroacoustics Conference, AIAA Paper 2005-2830, 2005.

[22] Bake, F., Michel, U., and Röhle, I., "Investigation of Entropy Noise in Aero-Engine Combustors," *Journal of Engineering for Gas Turbines and Power*, Vol. 129, No. 2, 2007, pp. 370–376. doi:10.1115/1.2364193

[23] Bake, F., Kings, N., and Röhle, I., "Fundamental Mechanism of Entropy Noise in Aero-Engines: Experimental Investigation," *Journal of Engineering for Gas Turbines and Power*, Vol. 130, No. 1, 2008, pp. 11202–12207. doi:10.1115/1.2749286

[24] Bake, F., Richter, C., Mühlbauer, B., Kings, N., Röhle, I., Thiele, F., and Noll, B., "The Entropy Wave Generator (EWG): A Reference Case on Entropy Noise," *Journal of Sound and Vibration*, Vol. 326, No. 3–5, Oct. 2009, pp. 574–598. doi:10.1016/j.jsv.2009.05.018

[25] Polifke, W., Paschereit, C., and Doebbeling, K., "Constructive and Destructive Interference of Acoustic and Entropy Waves in a Premixed Combustor with a Choked Exit," *International Journal of Acoustics and Vibration*, Vol. 6, No. 3, 2001, pp. 135–146.

[26] Eckstein, J., Freitag, E., Hirsch, C., and Sattelmayer, T., "Experimental Study on the Role of Entropy Waves in Low-Frequency Oscillations in a RQL Combustor," *Journal of Engineering for Gas Turbines and Power*, Vol. 128, No. 2, 2006, pp. 264–270. doi:10.1115/1.2132379

[27] McManus, K., Poinsot, T., and Candel, S., "A Review of Active Control of Combustion Instabilities," *Progress in Energy and Combustion Science*, Vol. 19, No. 1, 1993, pp. 1–29. doi:10.1016/0360-1285(93)90020-F

[28] Dowling, A. P., "The Calculation of Thermoacoustic Oscillations," *Journal of Sound and Vibration*, Vol. 180, No. 4, 1995, pp. 557–581. doi:10.1006/jsvi.1995.0100

[29] Moase, W., Brear, M., and Manzie, C., "The Forced Response of Choked Nozzles and Supersonic Diffusers," *Journal of Fluid Mechanics*, Vol. 585, No. 1, 2007, pp. 281–304. doi:10.1017/S0022112007006647

[30] Schmitt, P., Poinsot, T., Schuermans, B., and Geigle, K., "Large-Eddy Simulation and Experimental Study of Heat Transfer, Nitric Oxide Emissions and Combustion Instability in a Swirled Turbulent High Pressure Burner," *Journal of Fluid Mechanics*, Vol. 570, No. 1, 2007, pp. 17–46. doi:10.1017/S0022112006003156

[31] Poinsot, T., and Veynante, D., *Theoretical and Numerical Combustion*, 2nd ed., R. T. Edwards, Philadelphia, 2005.

[32] Moureau, V., Lartigue, G., Sommerer, Y., Angelberger, C., Colin, O., and Poinsot, T., "Numerical Methods for Unsteady Compressible Multi-Component Reacting Flows on Fixed and Moving Grids," *Journal of Computational Physics*, Vol. 202, No. 2, 2005, pp. 710–736. doi:10.1016/j.jcp.2004.08.003

[33] Childers, D. G., *Modern Spectrum Analysis*, IEEE, Piscataway, NJ, 1978.

P. Givi
Associate Editor